Desalination and Water Treatment
www.deswater.com
doi:10.5004/dwt.2021.27225

225 (2021) 311–319
June

Amidoxime functionalized hydroxyapatite composites separate the uranium(VI) from aqueous solution

Guojian Duan[a,*], Huining Tian[a], Hui Chen[a], Rong Wu[a], Zhen Xu[b], Tonghuan Liu[b], Xiaoxia Peng[a]

[a]*College of Pharmacy, Gansu University of Chinese Medicine, Lanzhou 730000, China, emails: duangj2004@126.com (G. Duan), 1842518203@qq.com (H. Tian), 2461976321@qq.com (H. Chen), wurong07260726@126.com (R. Wu), 1216105209@qq.com (X. Peng)*
[b]*Radiochemistry Laboratory & Key Laboratory of Special Function Material and Structure Design Dinistry Education, School of Nuclear Science and Technology, Lanzhou University, Lanzhou 730000, China, emails: xuzh14@lzu.edu.cn (Z. Xu), liuth@lzu.edu.cn (T. Liu)*

Received 14 January 2020; Accepted 5 March 2021

ABSTRACT

Amidoxime functionalized hydroxyapatite (HAP) composites were prepared and characterized by means of Fourier-transform infrared spectroscopy, scanning electron microscopy and X-ray powder diffraction. The adsorption characteristics of the adsorbent on uranyl ions were studied, and the effects of solid–liquid ratio, pH value, ionic strength, temperature, equilibrium time and other factors on the adsorption process were investigated. Under the optimum conditions, the adsorption capacity of the modified HAP material can reach 889.7 mg/g. The adsorption thermodynamics and kinetics data show that the adsorption of U(VI) by amidoxime (AO) functionalized hydroxyapatite is a spontaneous exothermic process, and the adsorption equilibrium can be reached within 30 min, which is in line with the Langmuir isothermal adsorption model. AO-*co*-HAP has a very good selectivity for U(VI). The desorption rate of U(VI) can reach 97.88% in 0.15 M acid solution. Compared with the traditional separation method, this adsorbent has a wider range of raw materials and a lower cost of waste liquid treatment, so it has an excellent practical application value.

Keywords: Adsorption; Amidoxime; Hydroxyapatite; Functionalized; U(VI)

1. Introduction

Uranium resources are the basis for the development of the nuclear industry. Under the background of the rapid development of nuclear power, the nuclear industry is facing the great challenge of resource shortage [1]. At the same time, for the waste liquid containing uranium, if improperly handled, the risk of uranium diffusion in water will be increased, which is the main reason for the potential threat of uranium to the ecosystem and human health. Therefore, the development of efficient separation and enrichment of U(VI) in radioactive waste liquid cannot only reduce its threat to the environment and human health, but also improve the utilization rate of nuclear fuel and reduce the cost of production and subsequent treatment, which is of great importance to the nuclear industry, especially the sustainable development of nuclear energy.

At present, the common enrichment and separation methods of uranyl ions are as follows: chemical precipitation [2], ion change [3], solvent extraction [4], membrane processes [5], chromatographic extraction [6], flotation and adsorption [7,8], etc. Most of these methods suffer from technical, economic and health problems related to poor selectivity, long time of extraction and large quantity of hazardous materials used. Compared to these technologies, adsorption was proven to be one of the most effective methods due to its wide range of material sources, low cost, high adsorption

* Corresponding author.

selectivity and capacity. At present, various kinds of materials, such as chelating resins [9,10], biosorbent [11,12], carbon based materials [13,14], and inorganic adsorbents, for example hydrous TiO_2 [15], PbS [16] and other functionalized inorganic adsorbents [17–19], have been developed for uranium removal.

With the development of the study, more and more kind of organic adsorbent gained research in the field of extraction of uranium from aqueous solution. Especially, adsorbents containing amidoxime groups, which make chelate complexes with uranyl ions, are notable for the recovery of uranium from wastewater. This kind of polymers include important properties such as high capacity, high selectivity, and fast kinetics. In the other hand, the chelate complexes with uranyl ions can disintegrate in low acidity, and metal ions can be released back into the solution. Through research, it is found that poly(acrylamidoxime) is very suitable for the separation of uranyl ions from water system for the following reasons: (i) its selectivity towards uranium, (ii) high uranium loading capacity, (iii) good mechanical strength, and (iv) amidoxime (AO) can be anchored to different polymer matrices of various shapes and sizes [20,21].

Hydroxyapatite (HAP) defined with $Ca_{10}(PO_4)_6(OH)_2$ is a member of the apatite mineral family. HAP can be used in remediation of soil and water from industrial and nuclear wastes due to its ability to retain a variety of ionic species, especially heavy metals. Recently, Handley-Sidhu et al. [22] and Liu et al. [23], reported the biogenic-HAP is a suitable material for the remediation of metal contaminated waters and for storage of radio nuclides waste separately, of which the maximum adsorption capacity of fluorine-doped hydroxyapatite was reported as 755 mg/g. However, the characteristics of HAP exists in the form of white powder which limit its practical usage. But this limitation can be minimized by the use of HAP-polymer composites [24]. It has been found that the HAP-polymer composites may display more properties of an effective adsorbent than the bare mineral or microgels [25,26]. The combination of hydroxyapatite and amidoxime group will make their respective advantages complementary to each other.

At the same time, the economic viability of recovery of uranium from wastewater still critically depends upon the kinetics of adsorption of uranium in AO absorbents. Therefore, the major challenge for making uranium recovery economically viable is to develop an adsorbent that has a very high uranium adsorption rate. Experiments involving in the adsorption of uranium from water with amidoxime-functionalized hydroxyapatite indicate that it has a very high selectivity, strong adsorption ability and large loaded capacity for many metal ions, especially for U(VI) advantage over others. In previous works, we have reported the synthesis of poly(acrylic acid-*co*-hydroxyapatite) composite and polyacrylic acid microgel for removing U(VI) [27,28]. As part of our continuing investigation into the development of polymer composites involving metal ions, the concern of this investigation is to introduce amidoxime-functionalized hydroxyapatite composite as adsorbent for adsorption of U(VI) from solutions. For the purpose of investigate the adsorption performance, the adsorption isotherm and parameters in the procedure were determined. The influence of experimental conditions such as solution pH value, initial U(VI) concentration and adsorption kinetic were studied. The attached U(VI) can be desorbed from this adsorbent by a small amount of inorganic acid.

2. Materials and methods

2.1. Materials

The hydroxyapatite was synthesized by calcium hydroxide (98%), phosphoric acid (99%), *N*,*N*-methylene-bis-acrylamide (Sinopharm Chemical Reagent Co., Ltd., China) and potassium persulfate (99.5%, Xi'an Reagent, China). The acrylonitrile was received from chemical reagent, Shanghai. Arsenazo-III (disodium salt) were obtained from Tianjin, China. Uranyl nitrate stock solution was prepared by dissolving uranyl nitrate hexahydrate ($UO_2(NO_3)_2{\cdot}6H_2O$) in deionized water. All the other chemicals were of analytical grade and deionized water was used unless stated otherwise. The pH of the working solution was adjusted to the desired value by the addition of 0.5 M HNO_3 or 0.5 M NaOH aqueous solutions.

2.2. Preparation of polyacrylonitrile-co-hydroxyapatite/amidoxime-functionalized hydroxyapatite (AN-co-HAP/AO-co-HAP)

AN-*co*-HAP composites was synthesized according to procedures reported by our previous research [28]. AO-*co*-HAP were prepared by adding 25 mL of 0.3 M H_3PO_4 to 50 mL of 0.25 M $Ca(OH)_2$ while stirring at 55°C for 15 min. Then adding different amount of acrylonitrile (HAP:AN = 8:1~1:8). Finally, *N*,*N*'-methylene-bis-acrylamide was added to propagate polymerization. Adding hydroxylamine hydrochloride solution at 70°C and the pH of the working solution was adjusted to the desired value by the addition of Na_2CO_3 aqueous solution. The entire reaction was carried out under a nitrogen atmosphere. The product were washed with deionized water until the unreacted substance were completely removed, followed by drying in a vacuum chamber. The product was ground and sieved down to 200 mesh size. The samples were characterized by means of attenuated total Fourier-transform infrared spectroscopy (FTIR), scanning electron microscopy (SEM) and X-ray powder diffraction analysis (XRD).

2.3. Determination of U(VI) in solution

The concentration of U(VI) was analyzed with the Arsenazo-III spectrophotometer method on a Shimadzu UV-723N spectrophotometer. 1 mL U(VI) solution sample, 1 mL 0.5 M HCl and 2 mL 1 g/L Arsenazo-III aqueous solution were added to a 25 mL volumetric flask, respectively. The glass flask was filled to 25 mL with deionized water. Shaking for 5 min and set aside for 15 min. The absorbance of the mixture liquid was measured at 650 nm [28].

2.4. Adsorption experiments

2.4.1. Adsorption capacity

The adsorption experiments were performed to investigate the process of adsorption of U(VI) from aqueous solution onto AO-*co*-HAP. Generally, a specified quantity of

AO-*co*-HAP, $NaNO_3$ and U(VI) stock solution was added into a polyethylene tubes with 10 mL of U(VI) solution or multi-ion-mixed solution at a given pH. Then shaking the mixture solution for 2 h in a thermostatic shaker bath under 25°C. The initial and the residual concentration of uranium were analyzed by UV-vis UV-723N spectrophotometer with Arsenazo-III as the complex agent at 650 nm [28]. Varying initial adsorbent dose, pH value, ionic strength and U(VI) concentration to observe the effects of different influence factors on the adsorption. The amounts of adsorbed ions q_e (mg/g), q_t (mg/g) and the percentage adsorption on the microgels (Adsorption%) were calculated according to the following equations:

$$q_e = \frac{(C_0 - C_e)V \times M_{U^{238}} \times 1{,}000}{m} \quad (1)$$

$$q_t = \frac{(C_0 - C_t)V \times M_{U^{238}} \times 1{,}000}{m} \quad (2)$$

$$\text{Adsorption}\,\% = \frac{C_0 - C_e}{C_0} \times 100\% \quad (3)$$

where C_0 and C_e are the liquid-phase concentrations of U(VI) at initial and equilibrium time (mol/L), respectively; V is the volume of the solution (L); m is the weight of dry adsorbent used (g).

In the aspect of economical technology regeneration of the adsorbent is very important [29]. 100 mg/L U(VI) was loaded onto AO-*co*-HAP was filtered and washed. Desorption studies were carried out with different concentrations of HNO_3 solution. To better understand the selectivity of AO-*co*-HAP towards U(VI), Ca^{2+}, Mg^{2+}, Sr^{+}, Pb^{2+}, Cu^{2+}, Co^{2+}, Ni^{2+} and Cd^{2+} were chosen as the interfering ions. When studying selective adsorption of AO-*co*-HAP, the concentrations of U(VI) and other metal ions in supernatants were determined by atomic adsorption spectroscopy.

2.4.2. Adsorption isotherm

The adsorption isotherm study is carried out by different volume of U(VI) solution shaken with certain adsorbent at different temperature for 2 h. Then the solution centrifuged at 10,000 rpm for 30 min at room temperature. The adsorption data for U(VI) were analyzed by a regression analysis which fits the Langmuir and Freundlich models. These data were plotted as a function of the amount of U(VI) bonded to the AO-*co*-HAP, at equilibrium vs. the U(VI) valuable metal concentration of the solution at equilibrium. The coefficients of the model were computed with linear least-square fitting [27].

3. Results

3.1. Characterization of the amidoxime-functionalized hydroxyapatite

3.1.1. FTIR spectra

The samples were characterized using FTIR (Perkin Elmer spectrum 100, USA) in pressed KBr pellets. The result is shown in Fig. 1.

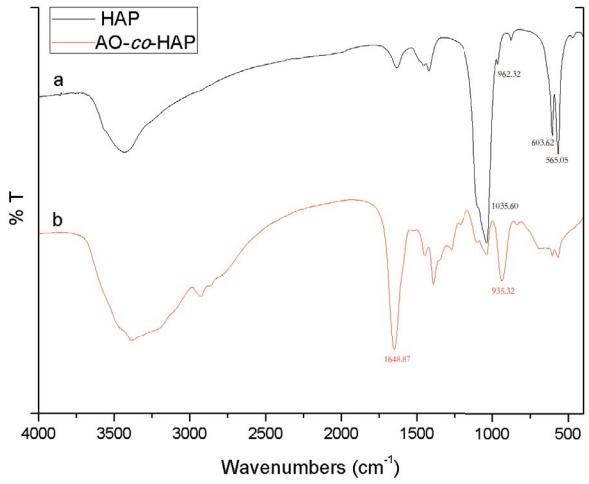

Fig. 1. FTIR spectra of HAP (a) and AO-*co*-HAP (b).

Fig. 1a can be seen the absorption at 1,035.60 cm^{-1} is due to the P=O associated stretching vibration. The P=O associated stretching vibration in PO_4^{3-} ions at 962.32 cm^{-1} is observed, the absorption peak at 603.62 cm^{-1} is due to the O–P–O asymmetric stretching vibration in the PO_4^{3-} group. The band located at 565.05 cm^{-1} can be assigned to the P–O mode of the PO_4^{3-} [29]. After modification with amidoxime groups (Fig. 1b), the appearance of new band at 1,648.87 is assigned to C=N and oxime groups stretching, respectively [30,31]. The peeks at 935.32 cm^{-1} is attributed to the N–O stretching vibration peak. FTIR experiments proved that amidoxime groups were successfully grafted on the structure of hydroxyapatite.

3.1.2. Scanning electron microscopy

The morphology of HAP and AO-*co*-HAP samples were characterized by SEM and the results are shown in Fig. 2.

As shown in Fig. 2a, morphology of HAP exhibited coarse, poriferous surface and of lax structure. But the image of AO-*co*-HAP (Fig. 2b) clearly exhibits favorable monodispersity in the sample. The average diameter of the particles ranges about 300 nm. The difference between Figs. 2a and b is a clear evidence of the obvious change in HAP morphology by the introduction of oximido groups. SEM results indicates that polymerization somehow diminished the mineral particles due to the amorphous contribution of oximido groups, thus predicting that adsorption of metal ions should increase due to the expansion of surface area by providing wider exposed sites for adsorption [32].

3.1.3. X-ray powder diffraction analysis

XRD can investigate the phase structure of the product. XRD was performed with Cu Kα radiation (k = 0.1541 nm) with a Rigaku X-ray diffractometer. XRD pattern of AO-*co*-HAP is distinctly revealed in Fig. 3. It is well known that the XRD peak intensities, peak shapes, and peak positions, which reflect the extent of crystallinity of the hydroxyapatite. The AO-*co*-HAP sample showed slightly broader and

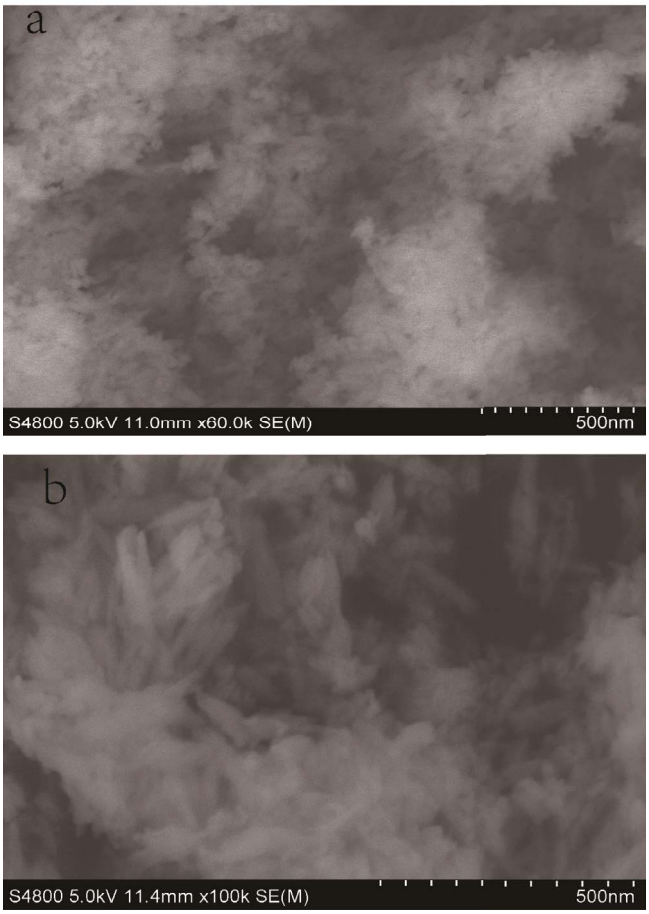

Fig. 2. SEM images of HAP (a) and AO-*co*-HAP (b).

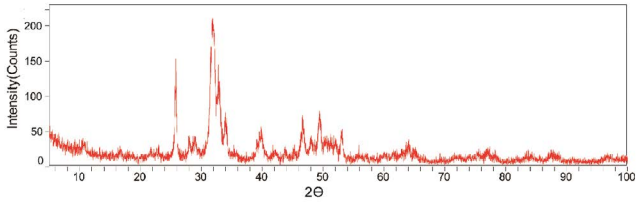

Fig. 3. XRD pattern of AO-*co*-HAP.

weaker XRD peaks compared to pure HAP [23]. From Fig. 3 we can see that the AO-*co*-HAP powders consist of crystalline phases [33], it is in conformity with the database completely. The major diffraction peaks at 2θ values of 25.8°, 31.9°, 32.4°, 34.1°and 39.8°, belong to HAP which match the JCPDS cards and in accordance with Franklin and Guhanathan [34].

3.2. Results of adsorption experiments

3.2.1. Effect of solid–liquid ratio (m/V)

In order to determine the optimum adsorbent amount, experimental data regarding the variation of distribution coefficient vs. the adsorbent mass were collected for U(VI). Batch equilibrium experiments were performed to test the

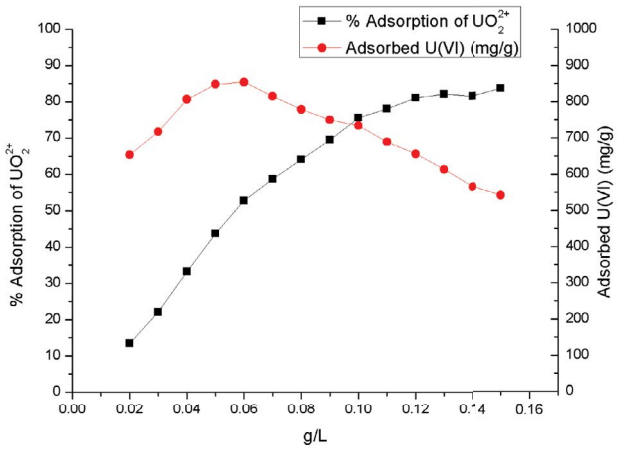

Fig. 4. Effect of adsorbent dose on U(VI) adsorption by AO-*co*-HAP (m/V = 0.1 g/L) ($[U(VI)]_0 = 4.03 \times 10^{-4}$ mol/L; pH = 4.00 ± 0.05; T = 298.15 ± 1.00 K; $C(NaNO_3)$ = 0.5 mol/L).

effectiveness of amidoxime-functionalized hydroxyapatite to recover U(VI) in water. The effect of adsorbent dose on U(VI) with a concentration of 4.03×10^{-4} mol/L removal from water sample was studied at different adsorbent dose ranging from 0.02 to 0.15 g/L at 298.15K.

In previous studies on hydroxyapatite, we obtained important results on the adsorption mechanisms, uranium is located in Ca sites of the hydroxyapatite [26]. It can be seen from the results (Fig. 4) that the amount of uranyl ions adsorbed increases with the increase of the mass of adsorbent when the adsorbent dose in the range of 0.02 to 0.15 g/L. The adsorption capacity to U(VI) reached the maximum value when the adsorbent dose is 0.13 g/L. However, when the solid–liquid ratio is 0.06 g/L, the adsorption efficiency of the adsorbent is the highest, and the q_e value can reach 854.3 mg/g. This may be because under given conditions, the solid–liquid ratio of the adsorbent, the concentration of uranyl ions, and the adsorption capacity of the adsorbent are well balanced, so that the adsorption capacity of the adsorbent can be maximized. However, with the increase of the ratio of solid to liquid, more adsorbents are involved in the adsorption of uranyl ions, making the adsorption percentage increase continuously until the ratio of solid to liquid is 0.13 g/L, and the equilibrium between uranyl ions in aqueous solution and the adsorbed uranyl ions reaches.

3.2.2. Effect of pH value

The pH value is usually an important factor affecting the recovery of U(VI) from radioactive waste liquid by adsorbents. Because the pH of the solution affects not only the surface chemistry of the polymer, but also the solution chemistry of soluble metal ions [35]. Therefore, in this paper, the pH value of the aqueous solution is in the range of 2.0–7.0 to conduct an experimental study on the adsorption capacity of the adsorbent to uranyl ions (Fig. 5).

When the aqueous solution is highly acidic, the adsorbent repels the positively charged U(VI) in the solution due to the protonation effect on its surface, so the adsorption efficiency under this condition is low. With the increase of

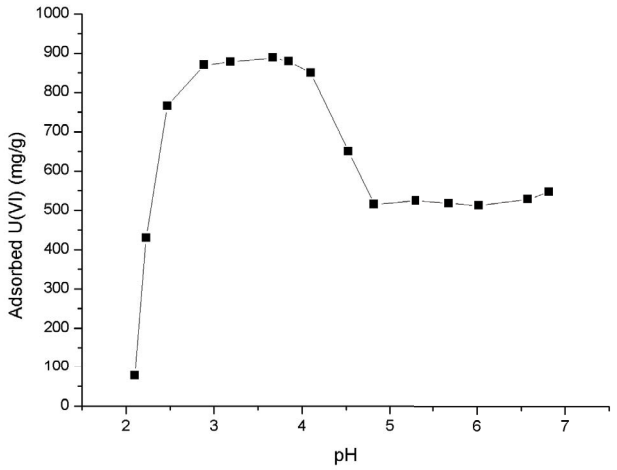

Fig. 5. Effect of pH on U(VI) adsorption by AO-*co*-HAP ($[U(VI)]_0$ = 4.03 × 10^{-4} mol/L; $C(NaNO_3)$ = 0.5 mol/L; T = 298.15 ± 1.00 K; t = 2 h; m/V = 0.10 g/L).

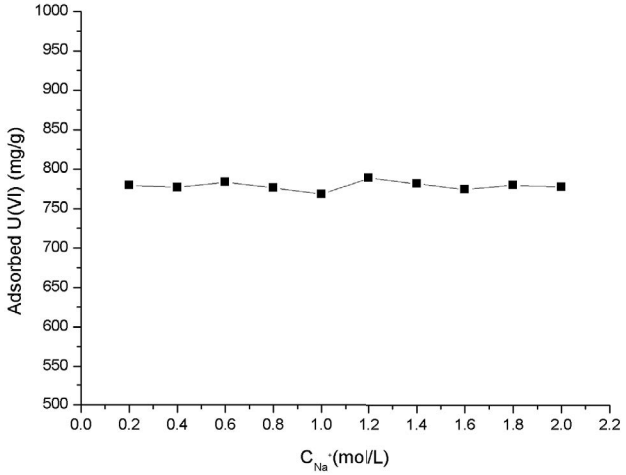

Fig. 6. Influence of ionic strength on U(VI) adsorption by AO-*co*-HAP ($[U(VI)]_0$ = 4.03 × 10^{-4} mol/L; pH = 4.00 ± 0.05; T = 298.15 ± 1.00 K; t = 2 h; m/V = 0.10 g/L).

pH value of the solution, the surface deprotonation of the adsorbent was significantly enhanced, and its swelling ability was improved accordingly. Under the combined action of the above two reasons, more and more active sites were used to bind to uranyl ions, thus rapidly enhancing the adsorption capacity of the adsorbent. Therefore optimum pH range for the removal of U(VI) from solution by AO-*co*-HAP were found to be between 3.0 to 4.0, and the maximum adsorption capability is 889.7 mg/g. If the pH value is greater than 4.0, the existence form of uranium changes due to the hydrolysis reaction of uranium in solution. At the same time, when the pH value is high, AO-*co*-HAP will also appear weak dissolution phenomenon. The comprehensive results show that when the pH value is greater than 4, the adsorption capacity of the adsorbent will be significantly reduced, but the q_e value will immediately remain between 450–500 mg/g. So, subsequent experiments were carried out under the condition that the pH value of the aqueous solution was equal to 4.0.

3.2.3. Effect of ionic strength

Fig. 6 shows the effect of ionic strength on the adsorption of U(VI) onto AO-*co*-HAP. The results indicate that the concentration of Na^+ was not show notable effects in the adsorption of U(VI) by AO-*co*-HAP, this is in consistent with the results obtained by others and our previous researchers [27,28]. While the ions strength in the waste or environmental water are normally not above 0.2 mol/L, so adsorption capability of AO-*co*-HAP to U(VI) can't be affected by the common metal salts concentration.

3.2.4. Effect of contact time and adsorption kinetics

Under the conditions as following: adsorbent dose is 0.10 g/L, pH value 4.00 and temperature 298.15 K, batch experiments were performed with a range shaking time of 1~120 min, and Fig. 7 shows the adsorption kinetics of U(VI) on AO-*co*-HAP. The adsorption rate was relatively fast, and the time required to reach equilibrium was in 30 min.

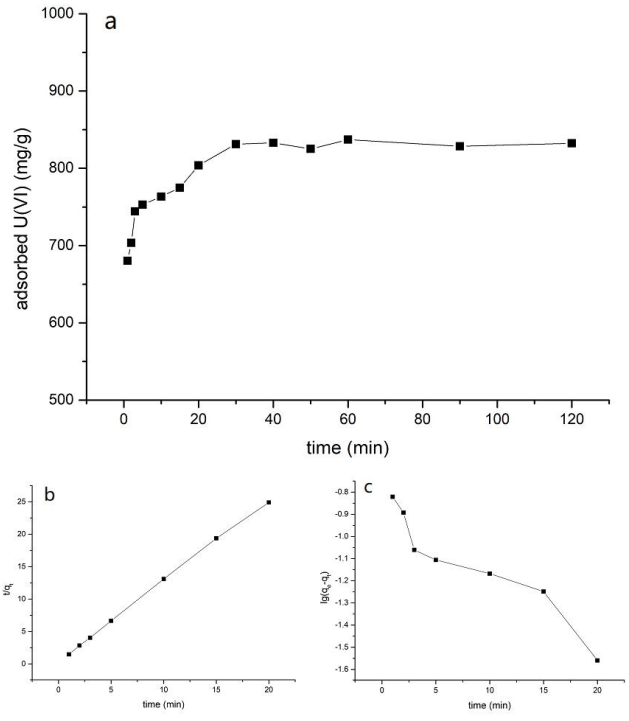

Fig. 7. Effect of contact time (a) and the pseudo-first-order (b), the pseudo-second-order (c) of U(VI) adsorption ($[U(VI)]_0$ = 4.03 × 10^{-4} mol/L; pH = 4.00 ± 0.05; T = 298.15 ± 1.00 K; $C(NaNO_3)$ = 0.5 mol/L; m/V = 0.10 g/L).

The short equilibrium time is attributed to the strong chelation of U(VI) with amidoxime functional groups and the PO_4^{3-} ions of AO-*co*-HAP which contributed to fast diffusion. Based on the kinetic data, AO-*co*-HAP may have good potentialities for real application in adsorbing U(VI) from large volumes of aqueous solutions. Adsorption kinetics of AO-*co*-HAP to U(VI) made up of two stages: an initial rapid

section where adsorption was fast and contributed significantly to equilibrium uptake, and a slower second section whose contribution to the total metal adsorption was relatively small. This indicates that there are a large number of hydroxyl and oxime groups in the structure of AO-*co*-HAP, which makes the adsorption process in the initial stage very fast. This results also proved that the adsorption mechanism of uranium on AO-*co*-HAP is mainly chemisorption reaction or strong surface complexation [35]. After 30 min, the change of adsorption capacities of AO-*co*-HAP did not show notable effects. In order to ensure the accuracy of this experiment, the balance time of subsequent adsorption experiments were set at 120 min.

In order to investigate the underlying adsorption mechanism of the sorption process further, pseudo-first and pseudo-second-order models were selected to evaluate the experimental data in this work. The pseudo-first kinetic model is given as [36]:

$$\ln(q_e - q_t) = \ln q_e - k_1 t \tag{4}$$

The pseudo-second kinetic model is given as [35]:

$$\frac{t}{q_t} = \frac{1}{k_2 q_e^2} + \frac{t}{q_e} \tag{5}$$

where T is the experiment temperature, q_e and q_t (mg/g) is the amount of uranium adsorbed at equilibrium and at time (t), k_1, k_2 is the rate constant of pseudo-first-order and pseudo-second-order kinetic model parameter, respectively.

The results of the kinetic parameters are shown in Table 1 and Fig. 7. As can be seen, the correlation coefficients R^2, obtained from the second-order equation exhibited a greater values compared to that of the first order equation. Moreover the adsorbed U(VI) amounts estimated from the second-order model closer to the experimental values when compared to that obtained from the first-order model. These results indicate that the kinetic data of the studied adsorption system fit better with the second-order kinetic model, which may give evidence that the chelation and complexation involving the share of electrons between the active sites of the microspheres adsorbent and the U(VI) ions is the rate limiting step [36].

3.2.5. Effect of temperature and thermodynamic data

The adsorption isotherm can be approximately expressed as a mathematical equation when it obeys an adsorption model. The equilibrium experiments were performed with samples of varying initial U(VI) concentration, and the pH value was selected at 4.0 in order to avoid the occurrence of insoluble U(VI) species. In order to study the adsorption isotherm, the Langmuir was used to describe the equilibrium adsorption isotherms, affording the most important parameter for designing a desired adsorption models had been successfully applied to describe the adsorption processes. Generally, the Langmuir isotherm model assumes that the sorption occurred on homogeneous surface by monolayer sorption, and there is no interaction between the adsorbates on adjacent sites. The expression of the Langmuir model is given as Eq. (6) [37]:

$$\frac{C_e}{q_e} = \frac{C_e}{q_{\max}} + \frac{1}{K_L q_{\max}} \tag{6}$$

where C_e is the equilibrium concentration of the U(VI) in the solution, q_e is the amount of U(VI) adsorbed at equilibrium, $q_{\max}$ is the maximum adsorption capacity of U(VI) (mg/g) and K_L is the Langmuir constant (L/mg) which correspond to the adsorption energy and binding sites affinity.

Generally, the Freundlich equation is an empirical equation. The linear equation for the Freundlich isotherm is given in Eq. (7):

$$\ln q_e = \ln K_F + \frac{1}{n} \ln C_e \tag{7}$$

where K_F and n are empirical constants those indicate the relative adsorption capacity and sorption intensity, respectively.

The results obtained from the fit of the data within the aforementioned mathematical models were collected in Table 2. As can be seen, the results shows that Langmuir isotherm model is the best model for describing the adsorption process with R^2 values > 0.99 compared to the Freundlich model, which means that the monolayer Langmuir adsorption model is better description in the adsorption of U(VI) onto amidoxime-functionalized AO-*co*-HAP.

The thermodynamic parameters include the change of Gibbs free energy, enthalpy and entropy of the adsorption process is calculated with the following equation [38]:

$$\ln K_d = \frac{\Delta S^\circ}{R} - \frac{\Delta H^\circ}{RT} \tag{8}$$

Table 1
Kinetic parameters derived from the pseudo-first-order and the pseudo-second-order model

Pseudo-first-order	Value	Pseudo-second-order	Value
q_e (g/g)	0.1356	q_e (g/g)	0.8043
R^2	0.8988	R^2	0.9993
k_1	0.0733	k_2	4.0521

Table 2
Freundlich isotherm model and Langmuir isotherm model constants

Isotherm model	Value
Freundlich model	
K_F (g/g)	8.1283
n	4.057
R^2	0.9156
Langmuir model	
$q_{\max}$ (g/g)	1.3497
b (L/mol)	18523
R^2	0.997

where K_d is the distribution coefficient, T is the adsorption temperature at which the processes are carried out, R is the gas constant (R = 8.314 J/mol K). The values of $\Delta H°$ and $\Delta S°$ were calculated from the slopes and intercepts of the linear variation of $\ln K_d$ vs. $1/T$.

The Gibbs free energy of specific adsorption $\Delta G°$ was calculated as the following equation [38]:

$$\Delta G° = \Delta H° - T\Delta S° \quad (9)$$

The values of $\Delta H°$ and $\Delta S°$ are listed in Table 3 which were calculated from linear plot of vs. $1/T$ using Van't Hoff equation (Eq. (8)), and the values of $\Delta G°$ were obtained using Eq. (9). The enthalpy ($\Delta H° > 0$) and entropy ($\Delta S° > 0$) changes for adsorbents and U(VI) ions show that the process of the adsorption was endothermic and the randomness in the solid-solution interface increased along with the adsorption process. The Gibbs free energy ($\Delta G° < 0$) indicates that the adsorption process was spontaneous, and the decrease of $\Delta G°$ values with temperature increasing shows that the sorption process was more favorable at higher temperature [39].

3.2.6. Desorption

Measuring the desorption capacity of adsorption materials is a very important process to determine its practical application value, and the desorption research results are helpful to verify the mechanism of adsorption process [40]. If the uranyl ion with positive charge can be separate with the adsorbent under neutral conditions, it indicates that they are combined by weak bonds, or even simple physical adsorption. If desorption can only be realized under acidic conditions, it indicates that uranyl ions are likely to form ionic bonds or even coordination bonds with adsorbent materials through ion exchange [39]. In this experiments, desorption efficiency of the amidoxime-functionalized hydroxyapatite was checked by HNO_3 solution with the concentration vary from 0.02 to 0.45 M. The results are shown in Fig. 8.

The results show that when the concentration of HNO_3 is very low, the desorption rate of uranyl ion is very low; with the increase of acid concentration, the desorption rate of uranyl ion increases rapidly. When the concentration of nitric acid is 0.15 M, the desorption rate of uranyl ion can reach 97.88%. This result is consistent with the effect of pH value on the adsorption process. The experimental results show that amidoxime-functionalized hydroxyapatite has a good practical application potential in the treatment of uranyl ions in radioactive waste liquid.

Table 3
Thermodynamic parameters

Temperature (K)	$\Delta H°$ (kJ/mol)	$\Delta S°$ (J/mol K)	$\Delta G°$ (kJ/mol)
98.15	4.4242	52.9	–11.3479
303.15	4.4242	52.9	–11.6124
308.15	4.4242	52.9	–11.8769
313.15	4.4242	52.9	–12.1414

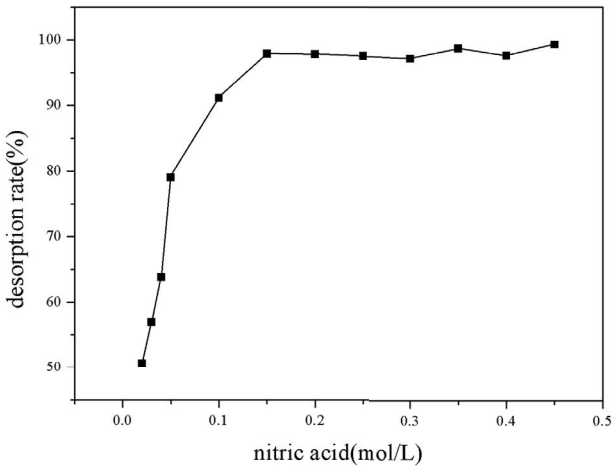

Fig. 8. Desorption efficiency of U(VI) as a function of HNO_3 acid concentration (C($NaNO_3$) = 0.5 mol/L; T = 298.15 ± 1.00 K; t = 2 h; m/V = 0.10 g/L).

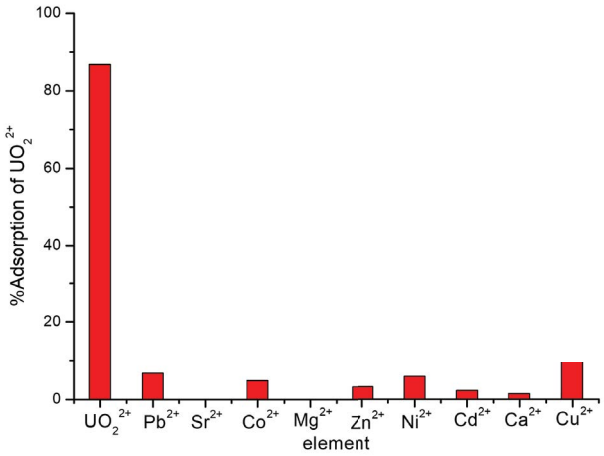

Fig. 9. Selectivity of U(VI) onto AO-*co*-HAP (C($NaNO_3$) = 0.5 mol/L; T = 298.15 ± 1.00 K; t = 2 h; m/V = 0.10 g/L).

3.2.7. Selectivity

Generally, there are various types of metal ions in radioactive industrial wastewater, and the coexisting ions will affect the binding of the specified ions with adsorbents, and also reduce the adsorption capacity of the adsorption material to the target ions. Therefore, the selectivity of the adsorbent is a very important factor. To better understand the selectivity of AO-*co*-HAP to uranyl ion, we selected Pb^{2+}, Cu^{2+}, Co^{2+}, Zn^{2+}, Ni^{2+}, Cd^{2+}, Ca^{2+}, Mg^{2+}, Sr^{2+} as coexisting ions. In this experiment, all the initial concentrations were fixed at 3.267×10^{-4} mol/L. In the presence of various metal ions, the concentrations of various metal ions in the solution before and after adsorption were determined for calculation and comparison. The results are shown in Fig. 9. The results indicate that the adsorbent exhibited good adsorption selectivity for uranyl ion rather than the other elements mentioned above. The outstanding selectivity is mainly attributed to the following reasons:

(1) the amidoxime groups of AO-*co*-HAP are the reactive basic centers that contribute directly to the adsorption and combined with uranyl ion in the form of chelate. (2) The average U–N bond distances are significantly shorter than the corresponding distances in other metal-nitrogen bonds, leading to a strong tendency of nitrogen-containing functional groups toward U(VI) ions [38]. The combination of these two factors makes AO-*co*-HAP have excellent selectivity for uranyl ions.

4. Conclusions

In this paper, the organic/inorganic composites of amidoxime functionalized hydroxyapatite were prepared by free radical polymerization method. The structural characterization results showed that the prepared amidoxime functionalized hydroxyapatite had a more orderly structure than the single hydroxyapatite. From the analysis of the experimental results of various factors affecting the adsorption process, it can be seen that the optimal adsorption conditions of AO-*co*-HAP for uranyl ions are as follows: pH value of the solution system is equal to 4, solid–liquid ratio is 0.06 g/L, ionic strength has almost no effect on the adsorption process, and the maximum adsorption capacity of AO-*co*-HAP for uranyl ions can reach 889.7 mg/g. This adsorption process can reach equilibrium within 30 min. Thermodynamic and kinetic data show that the adsorption of U(VI) by amidoxime functionalized hydroxyapatite is a spontaneous exothermic process, which follows the second-order kinetics and adsorption isotherm, and conforms to the Langmuir isotherm adsorption model. The results of desorption experiments show that the desorption rate of AO-*co*-HAP to uranyl ion can reach 97.88% in 0.15 M HNO_3 aqueous solution. The results of selective experiments also verify the excellent selectivity of amidoxime group to uranyl ions. Amidoxime functionalized hydroxyapatite realized the selective adsorption of amidoxime group to uranyl ions and the superior combination of large specific surface area of hydroxyapatite. At the same time, the raw material of this kind of adsorbent is cheap and easy to obtain, and the cost of synthesis and treatment is low, which makes it have a good practical application potential in enrichment and separation of U(VI) from radioactive waste liquid.

Author contributions

Writing—original draft preparation, Guojian Duan; writing—review and editing, Tonghuan Liu; project administration, Guojian Duan; data curation, Hui Chen, Rong Wu; reagents/materials/analysis tools, Huining Tian, Zhen Xu, Xiaoxia Peng; funding acquisition, Guojian Duan.

Funding

This research was funded by National Natural Science Foundation of China (No. 21762001); Key Scientific Research Projects of Gansu Institute of Traditional Chinese Medicine (No. 2305137401).

References

[1] S.-H. Choi, M.-S. Choi, Y.-T. Park, K.-P. Lee, H.-D. Kang, Adsorption of uranium ions by resins with amidoxime and amidoxime/carboxyl group prepared by radiation-induced polymerization, Radiat. Phys. Chem., 67 (2003) 387–390.
[2] A. Mellah, S. Chegrouche, M. Barkat, The precipitation of ammonium uranyl carbonate (AUC): thermodynamic and kinetic investigations, Hydrometallurgy, 85 (2007) 163–171.
[3] J.T.M. Amphlett, M.D. Ogden, R.I. Foster, N. Syna, K.H. Soldenhoff, C.A. Sharrad, The effect of contaminants on the application of polyamine functionalized ion exchange resins for uranium extraction from sulfate based mining process waters, Chem. Eng. J., 354 (2018) 633–640.
[4] K.C. Pitchaiah, K. Sujatha, J. Deepitha, S. Ghosh, N. Sivaraman, Recovery of uranium and plutonium from pyrochemical salt matrix using supercritical fluid extraction, J. Supercrit. Fluids, 147 (2019) 194–204.
[5] S.D. Kolev, A.M. St. John, R.W. Cattrall, Mathematical modeling of the extraction of uranium(VI) into a polymer inclusion membrane composed of PVC and di-(2-ethylhexyl) phosphoric acid, J. Membr. Sci., 425–426 (2013) 169–175.
[6] J.A. Drader, L.P. Zhu, P. Smith, K. McCann, S. Boyes, J.C. Braley, Assessment of monoamide extractants and solid supports as new extraction chromatographic materials, Sep. Purif. Technol., 163 (2016) 352–356.
[7] Y.J. Jung, S. Kim, S.-J. Park, J.M. Kim, Application of polymer-modified nanoporous silica to adsorbents of uranyl ions, Colloids Surf., A, 313–314 (2008) 162–166.
[8] T. Tsuruta, Biosorption of uranium for environmental applications using bacteria isolated from the uranium deposits, Microbes Microbial Technol., 11 (2011) 267–281.
[9] E. Serpil, P. Erol, Evaluation of chelate and cation exchange resins to remove copper ions, Powder Technol., 301 (2016) 520–525.
[10] G.J. Duan, T.H. Liu, W.S. Wu, Y. Yang, Adsorption of UO_2^{2+} from aqueous solution onto copolymers of styrene and maleic anhydride, J. Radioanal. Nucl. Chem., 295 (2013) 2193–2201.
[11] A.-M. Lakaniemi, G.B. Douglas, A.H. Kaksonen, Engineering and kinetic aspects of bacterial uranium reduction for the remediation of uranium contaminated environments, J. Hazard. Mater., 371 (2019) 198–212.
[12] K.H. Williams, J.R. Bargar, J.R. Lloyd, D.R. Lovley, Bioremediation of uranium-contaminated groundwater: a systems approach to subsurface biogeochemistry, Curr. Opin. Biotechnol., 24 (2013) 489–497.
[13] M.E. Mahmoud, M.A. Khalifa, Y.M. El Wakeel, M.S. Header, R.M. El-Sharkawy, S. Kumar, T.M. Abdel-Fattah, A novel nanocomposite of Liquidambar styraciflua fruit biochar-crosslinked-nanosilica for uranyl removal from water, Bioresour. Technol., 278 (2019) 124–129.
[14] J. Jin, S.W. Li, X.Q. Peng, W. Liu, C.L. Zhang, Y. Yang, L.F. Han, Z.W. Du, K. Sun, X.K. Wang, HNO_3 modified biochars for uranium(VI) removal from aqueous solution, Bioresour. Technol., 256 (2018) 247–253.
[15] M.-J. López-Muñoz, A. Arencibia, L. Cerro, R. Pascual, Á. Melgar, Adsorption of Hg(II) from aqueous solutions using TiO_2 and titanate nanotube adsorbents, Appl. Surf. Sci., 367 (2016) 91–100.
[16] L.F. Rao, Application of radiation grafting: progress and status of the extraction of uranium from seawater in Japan, J. Isot., 25 (2012) 129–139 (in Chinese).
[17] T. Madrakian, A. Afkhami, M. Rahimi, Removal, preconcentration and spectrophotometric determination of U(VI) from water samples using modified maghemite nanoparticles, J. Radioanal. Nucl. Chem., 292 (2012) 597–602.
[18] F. Zahran, H.H. El-Maghrabi, G. Hussein, S.M. Abdelmaged, Fabrication of bentonite based nanocomposite as a novel low cost adsorbent for uranium ion removal, Environ. Nanotechnol. Monit. Manage., 11 (2019) 100205, doi: 10.1016/j.enmm.2018.100205.
[19] B. Liang, J.N. Nie, X.Q. Jiang, M.X. Song, F.Q. Dong, L.P. Shang, H. Deng, H.C. He, N. Belzile, Y.W. Chen, B. Xu, X.N. Liu, Selective adsorption of uranyl and potentially toxic metal ions at the core-shell Fe_2O_4-TiO_2 (M=Mn, Fe, Zn, Co, or Ni) nanoparticles, J. Hazard. Mater., 365 (2019) 835–845.

[20] G. Bayramoglu, M.Y. Arica, MCM-41 silica particles grafted with polyacrylonitrile: modification in to amidoxime and carboxyl groups for enhanced uranium removal from aqueous medium, Microporous Mesoporous Mater., 226 (2016) 117–124.
[21] G. Bayramoglu, M.Y. Arica, Star type polymer grafted and polyamidoxime modified silica coated-magnetic particles for adsorption of U(VI) ions from solution, Chem. Eng. Res. Des.,147 (2019) 146–159.
[22] S. Handley-Sidhu, J.C. Renshaw, S. Moriyama, B. Stolpe, C. Mennan, S. Bagheriasl, P. Yong, A. Stamboulis, M. Paterson-Beedle, K. Sasaki, R.A.D. Pattrick, J.R. Lead, L.E. Macaskie, Uptake of Sr^{2+} and Co^{2+} into biogenic hydroxyapatite: implications for biomineral ion exchange synthesis, Environ. Sci. Technol., 45 (2011) 6985–6990.
[23] J. Liu, C.S. Zhao, Z.B. Zhang, J.L. Liao, Y.H. Liu, X.H. Cao, J.J. Yang, Y.Y. Yang, N. Liu, Fluorine effects on U(VI) sorption by hydroxyapatite, Chem. Eng. J., 288 (2016) 505–515.
[24] D. Baybaş, U. Ulusoy, Polyacrylamide–hydroxyapatite composite: preparation, characterization and adsorptive features for uranium and thorium, J. Solid State Chem., 194 (2012) 1–8.
[25] A. Recep, Synthesis and characterization of poly(2-hydroxyethylmethacrylate-hydroxyapatite) a novel composite for the removal of lead(II) from aqueous solutions, Clean Soil Air Water, 40 (2012) 1257–1264.
[26] A. Recep, Separation of uranium and thorium in aqueous solution using poly hydroxyl ethyl methacrylate-hydroxyapatite novel composite, Desal. Water Treat., 50 (2012) 180–188.
[27] T.H. Liu, G.J. Duan, X.J. Duan, W.S. Wu, Y. Yang, Adsorption features of polyacrylic acid hydrogel for UO_2^{2+}, J. Radioanal. Nucl. Chem., 297 (2013) 119–125.
[28] T.H. Liu, Z. Xu, G.J. Duan, Y.P. Tan, Q.Q. Zhong, W.S. Wu, Adsorptive features of poly(acrylic acid-co-hydroxyapatite) composite for UO_2^{2+}, J. Radioanal. Nucl. Chem., 307 (2016) 1221–1230.
[29] M. Manso, M. Langlet, C. Jiménez, J.M. Martínez-Duart, Hydroxyapatite coatings obtained by the thermal activation of polymeric sols, Int. J. Inorg. Mater., 3 (2001) 1153–1155.
[30] N. Bilba, D. Bilba, G. Moroi, Synthesis of a polyacrylamidoxime chelating fiber and its efficiency in the retention of palladium ions, J. Appl. Polym. Sci., 92 (2004) 3730–3735.
[31] G. Bayramoglu, M.Y. Arica, Amidoxime functionalized *Trametes trogii* pellets for removal of uranium(VI) from aqueous medium, J. Radioanal. Nucl. Chem., 307 (2015) 373–384.
[32] G. Bayramoglu, M.Y. Arica, Polyethylenimine and tris(2-aminoethyl)amine modified p(GA–EGMA) microbeads for sorption of uranium ions: equilibrium, kinetic and thermodynamic studies, J. Radioanal. Nucl. Chem., 312 (2017) 293–303.
[33] G. Singh, H. Singh, B.S. Sidhu, In vitro corrosion investigations of plasma-sprayed hydroxyapatite and hydroxyapatite-calcium phosphate coatings on 316L SS, Bull. Mater. Sci., 37 (2014) 1519–1528.
[34] D.S. Franklin, S. Guhanathan, Performance of silane-coupling agent-treated hydroxyapatite/diethylene glycol-based pH-sensitive biocomposite hydrogels, Iran. Polym. J., 23 (2014) 809–817.
[35] M. Monier, D.A. Abdel-Latif, Synthesis and characterization of ion-imprinted resin based on carboxymethyl cellulose for selective removal of UO_2^{2+}, Carbohydr. Polym., 97 (2013) 743–752.
[36] D. Robati, Pseudo-second-order kinetic equations for modeling adsorption systems for removal of lead ions using multi-walled carbon nanotube, J. Nanostruct. Chem., 3 (2013) 55, doi: 10.1186/2193-8865-3-55.
[37] C. Xu, J.J. Wang, T.L. Yang, X. Chen, X.Y. Liu, X.C. Ding, Adsorption of uranium by amidoximated chitosan-grafted polyacrylonitrile, using response surface methodology, Carbohydr. Polym., 121 (2015) 79–85.
[38] Z.-P. Cheng, Y.-H. Liu, G.-X. Xiong, X.-P. Luo, X.-H. Cao, M. Li, Z.-B. Zhang, Preparation of amidoximated polymer composite based on CMK-3 for selective separation of uranium from aqueous solutions, J. Radioanal. Nucl. Chem., 306 (2015) 365–375.
[39] D.Z. Yuan, L. Chen, X. Xiong, L.G. Yuan, S.J. Liao, Y. Wang, Removal of uranium(VI) from aqueous solution by amidoxime functionalized superparamagnetic polymer microspheres prepared by a controlled radical polymerization in the presence of DPE, Chem. Eng. J., 285 (2016) 358–367.
[40] T.S. Anirudhan, J.R. Deepa, Synthesis and characterization of multi-carboxyl-functionalized nanocellulose/nanabentonite composite for the adsorption of uranium(VI) from aqueous solutions: kinetic and equilibrium profiles, Chem. Eng. J., 273 (2015) 390–400.